Palaeomagnetic field strength variations suggest Mesoproterozoic inner core nucleation

Biggin, A.J.[1], Piispa, E.[2], Pesonen, L.J.[3], Holme, R.[1], Paterson, G.A.[4], Veikkolainen, T.[3], Tauxe, L.[5]

1. *Department of Earth, Ocean and Ecological Sciences, University of Liverpool, Liverpool L69 7ZE, UK.*
2. *Department of Geological and Mining Engineering and Sciences, Michigan Technological University, Houghton, 1400 Townsend Drive, MI 49931, USA.*
3. *Department of Physics, Division of Materials Physics, PB 64, FI-00014 University of Helsinki, Helsinki, Finland.*
4. *Key Laboratory of Earth and Planetary Physics, Institute of Geology and Geophysics, Chinese Academy of Sciences, Beijing 100029, China.*
5. *Scripps Institution of Oceanography, University of California San Diego, La Jolla, California 92093-0220 USA.*

The Earth's inner core grows by the freezing of liquid iron at its surface. The point in history at which this process initiated marks a step-change in the thermal evolution of the planet. Recent computational and experimental studies[1-5] have presented radically differing estimates of the thermal conductivity of the Earth's core resulting in widely ranged dates of inner core nucleation (from less than 0.5 to nearly 2 billion years). Some of these raise serious challenges to explaining how the dynamo responsible for generating the geomagnetic field has been sustained over the whole of observed Earth history. The nucleation of the core leads to a different convective regime[6], and might be expected to produce different magnetic field structures, producing an observable signal in the palaeomagnetic record and allowing the date of inner-core nucleation to be estimated directly. Previous studies searching for this signature have been hampered by the paucity of palaeomagnetic intensity measurements, by the lack of an effective means of assessing their reliability, and by shorter timescale geomagnetic variations. Here we examine results from an expanded Precambrian database of palaeomagnetic intensity measurements[7] selected using a new set of reliability criteria[8]. Our analysis provides the first intensity-based support for the dominant dipolarity of the time-averaged Precambrian field, a crucial requirement for palaeomagnetic reconstructions of continents. We also present the first firm evidence for the existence of very long-term variations in geomagnetic strength. The most prominent and robust transition in the record is an increase in both average field strength and variability observed to occur between 1 and 1.5 billion years ago. This observation is most readily explained by the nucleation of the inner core occurring during this interval[9]; the timing would tend to favour a modest value of core thermal conductivity and supports a simple thermal evolution model for the Earth.

Palaeomagnetists have long sought to use data to constrain the thermal evolution of Earth through its influence on the geodynamo[10-16]. In recent years, the quality and quantity of palaeomagnetic intensity (palaeointensity) measurements have increased dramatically allowing certain very long term variations in the Earth's dipole moment to be claimed alongside postulated causes. For example, a "Proterozoic Dipole Low" extending from earliest Proterozoic (ca. 2450 Myr ago) to at least Cambrian (ca. 500 Myr ago) times was argued to reflect a weakened state of the geodynamo prior to inner core nucleation providing a substantial new power source[7]. More recently, the minimum of this weak-field interval was argued to be much earlier at ca. 2300-1800 Myr ago[17] and potentially linked to the existence of a dynamo generated in a basal magma ocean just above the outer core. Both of these studies suffered from limitations that we set out to address here: a shortage of measurement data in crucial time periods and an inability to demonstrate that claimed features were robust against sources of bias that include the intrinsic variability of the magnetic field on timescales of tens of Myr and less, and the variable reliability of the measurement data.

The present study uses a global compilation of 363 palaeointensity data (17% more than used by ref. 17 and with 41% more data in the interval 1000 to 1500 Myr) from the PINT database (http://earth.liv.ac.uk/pint/) which have all been assigned palaeointensity quality (Q_{PI}) values[8]. These values, applied at the palaeomagnetic site mean level, reflects the total number (maximum nine, see *Methods*) of a set of individual criteria judged to have been met by a single palaeointensity estimate. For the purposes of this study, 43 estimates that had Q_{PI} values of 0 (or which were duplicates of other, higher quality, data) were excluded leaving 320 estimates from 36 studies (Supplementary Tables 1 and 2) for analysis.

Figure 1a,b shows the tendency of 118 of these palaeointensity results, selected because they were accompanied by suitable directional information (see *Methods*), to display a positive relationship between palaeointensity and palaeomagnetic inclination consistent with a dipole-dominated field. For $Q_{PI} \geq 1$-5, all intensity data have significant positive Kendall rank correlations with inclination ($\tau \geq 0.232$, $P \leq 0.0345$; see Methods). This result further supports the hypothesis that the geomagnetic field has been dipole-dominated for most of its history, previously only investigated for the Precambrian using directional data[18,19]. The scatter about a dipole fit, as measured by the standard deviation about the expected intensity for a given inclination, decreases markedly as the minimum Q_{PI} value of the points is increased from 2 through 4 (Figure 1c) strengthening this observation and suggesting that Q_{PI} criteria are an effective means of assessing Precambrian-aged palaeointensity data.

The time evolution of the dipole moment was assessed using datasets with various minimum Q_{PI} values (Figure 2, Extended Data Figures 1-4). A minimum Q_{PI} cut-off of 3 offers the optimal trade-off between misfit and quantity of data (Figure 1c) but datasets produced using different cut-offs are also consistent with the findings detailed below (see Supplementary Table 3).

Dipole moment estimates are far from uniformly distributed through the assessed time period (500-3500 Myr; Figure 2). Within the more densely populated central time interval (1000-2800 Myr), virtual (axial) dipole moment (V(A)DM) measurements tend to be distributed in “strips” of measurements made from units of individual igneous provinces with small differences in age. A large range of V(A)DM measurements within a few Myr or less is fully consistent with palaeomagnetic records from the last 2 Myr[20,21] supporting similar field behaviour throughout Earth history.

Similar to what is observed for the 0-200 Myr time period[22], V(A)DM measurements less than or equal to 50 ZAm^2 are ubiquitous in the Precambrian record (figure 2). By contrast “high” V(A)DM measurements (greater than 50 ZAm^2) are confined to time periods before 2400 Myr ago (denoted EARLY) and after 1300 Myr ago (denoted LATE). Some 48% of the estimates in these intervals (80 from a total of 166) are “high” versus just 5% (2 from 41) in the intervening interval (denoted MID). Systematic bias from non-ideal rock magnetic behaviour or experimental procedures is very unlikely to be responsible for this disparity: MID interval measurements are sourced from 12 distinct studies (Supplementary Table 2) performed on a variety of lithologies (lavas, dykes, and plutons). Similarly, "high" estimates from outside MID are sourced from 11 distinct studies from a total of 23 in the two intervals, also from a variety of lithologies. Although the potential for biasing of palaeointensity estimates by poorly understood processes may remain even for results with high Q_{PI} values[23-25], this could not explain higher estimates being commonplace in certain parts of the Precambrian but nearly absent in other parts that are otherwise reasonably well-represented.

Each dataset (EARLY, MID, and LATE) was analysed using non-parametric statistics (Figure 3, Extended Data figure 5 and Supplementary Table 3). The distributions of V(A)DMs with $Q_{PI} \geq 3$ in the LATE (median = 54 +3/-7 ZAm^2) and EARLY (median = 44 +6/-3 ZAm^2) intervals are distinct beyond the 90% confidence limit (P=0.064) according to the Kolmogorov-Smirnov test (Supplementary Table 3). MID has a median (30 ± 8 ZAm^2) which is 32% lower than EARLY and 44% lower than LATE and is distinct from both at a confidence limit >> 99.9%. The significance level of these disparities remains >99% using a minimum Q_{PI} cut-off of 4 and far exceeds this using cut-offs of 1 and 2 (Supplementary Table 3). A further resampling test (see *Methods*), incorporating quoted uncertainties in both the V(A)DMs and their associated ages also produces significant results for a Q_{PI} cut-off of 3 or below (Extended Data Table 1).

To investigate whether the differences observed between our intervals could be explained by oversampling of geomagnetic variations occurring on timescales shorter than those which we are interested in here, we devised a tailored likelihood test (see *Methods*). This incorporates effects of bias arising from large (factor of 3) and long-lasting (50 Myr, chosen to be longer than any known superchron) shifts in the time-averaged dipole (likely due to variable mantle forcing[26]) and also bias potentially caused by "normal" secular variation on the clustering of measurements, derived from the same suite of igneous rocks, within periods of 200 kyr. Analysing the data with $Q_{PI} \geq 3$ (Extended Data Table 2) indicates that, as would be expected, substantial differences between the distributions of V(A)DM data are much more likely to arise by chance when such sources of bias are considered. In particular, they could explain the differences observed between the V(A)DM distributions produced from the EARLY and MID intervals (P=0.187). Nevertheless, the simultaneous observation of differences of the same magnitude as observed between time periods MID and LATE remains highly unlikely (P=0.012) without appealing to either systematic measurement bias or some very long term evolution of the time-averaged dipole moment. Two studies[27,28] which were not fully represented in previous versions of the database contribute 72% of the data within the LATE interval. Nevertheless, arbitrarily excluding all data from either one of these studies still yields a low likelihood (P ≤ 0.068) that the differences observed exist by chance alone (Extended Data Table 2). Given that there is no good reason to suspect that both of them are biased high, we infer that the observed differences are robust. Similarly, robust results (though with reduced levels of significance) are produced if we allow the long term changes to increase to extreme factors of 6 and 12 (Extended Data Table 2). We conclude that our updated palaeointensity dataset presents the first compelling evidence of geomagnetic intensity variations occurring on timescales longer than those which have previously been ascribed to mantle convection. Furthermore, a significant increase in the time averaged dipole moment very likely did occur at some time close to the end of our MID interval or near the beginning of our LATE time interval. Interestingly, the timing of this transition fits well with a recent finding[29] that the pattern of palaeomagnetic secular variation (based on purely directional data) shifted to a less stable state ca. 1500 Myr ago.

Taken at face value, the record summarised in Figure 2d (and extended data figures 1d-4d) indicates that there was a gradual decrease in dipole moment and its variability beginning in the late Archaean (ca. 2500 Myr ago) which terminated with an abrupt increase in the Mesoproterozoic (ca. 1300 Myr ago). A qualitatively similar pattern of dipole moment evolution through the Precambrian was predicted by a study[9] employing a thermal evolution model coupled to the results of scaling analyses of numerical geodynamo models. In the framework of this "Low Power" end-member prediction (Figure 11b in ref. 9), the gradual decrease in dipole moment would reflect the diminishing vigour of thermal convection caused by the secular cooling of the core; the subsequent sharp recovery at ca. 1300 Ma would mark the sudden commencement of much more efficient compositional convection at the point of inner core nucleation. The thermal model in question predicted a somewhat earlier low-high transition (i.e. age of inner core nucleation) of ca. 1800 Myr ago but we speculate that a slightly less extreme "Low-Mid Power" model could show good agreement with the record presented here.

A corollary of a Mesoproterozoic-age inner core and a conventional thermal history of the Earth is that the long term dipole moment would likely have undergone only a small decrease since the onset of compositional convection[9]. Although intervening data are currently rare, a relative wealth of palaeointensity data is available in the interval 0-300 Myr ago and enables a limited test of this hypothesis. A high quality subset of these data (the RECENT interval, see *Methods*) yields a median V(A)DM (50 ± 5 ZAm^2) which is ≤ 10% lower than that of the LATE interval (Figure 3, Extended Data Figure 5 and Supplementary Table 3). Similarly, a recent analysis[22] of the last 200 Myr yielded a long term median dipole moment of 42 ZAm^2 which is a maximum of 24% lower than the median values calculated for our LATE interval. Thus the high values of dipole moment in our LATE interval are nearly matched by those within the RECENT interval consistent with the very-long-term strength of the field decaying only marginally since inner core nucleation. Our prediction is therefore supported by existing data and a more complete test will be possible in the future once the time period 300-1000 Myr has been populated with reliable new palaeointensity measurements.

Our interpretation of the dipole moment record is not unequivocal because the implications of inner core nucleation for the observable field at the Earth's surface are not fully understood. Furthermore, some mantle-forced shift in core-mantle heat flow, lasting in excess of 50 Myr and perhaps related to the supercontinent cycle or secular mantle evolution, cannot be ruled out as causing a significant shift in geomagnetic behaviour during the Mesoproterozoic. Nevertheless, in the absence of rival thermal models making predictions similar to that which we have based our interpretation on, we argue that nucleation of the inner core in the Mesoproterozoic is presently the most likely explanation for the increase we have reported. Alternative candidates, potentially worthy of testing with models in the future, include increases in core-mantle heat flow resulting from the onset of whole mantle convection (or even plate tectonics) and the first appearance of post-perovskite (with associated elevated thermal diffusivity[30]) at the base of the mantle.

References from main text

1 Pozzo, M., Davies, C., Gubbins, D. & Alfè, D. Thermal and electrical conductivity of iron at Earth's core conditions. *Nature* **485**, 355-358 (2012).

2 Seagle, C. T., Cottrell, E., Fei, Y. W., Hummer, D. R. & Prakapenka, V. B. Electrical and thermal transport properties of iron and iron-silicon alloy at high pressure. *Geophys Res Lett* **40**, 5377-5381, doi:10.1002/2013gl057930 (2013).

3 Gomi, H. *et al.* The high conductivity of iron and thermal evolution of the Earth's core. *Phys Earth Planet In* **224**, 88-103, doi:10.1016/j.pepi.2013.07.010 (2013).
4 de Koker, N., Steinle-Neumann, G. & Vlcek, V. Electrical resistivity and thermal conductivity of liquid Fe alloys at high P and T, and heat flux in Earth's core. *P Natl Acad Sci USA* **109**, 4070-4073, doi:10.1073/pnas.1111841109 (2012).
5 Zhang, P., Cohen, R. E. & Haule, K. Effects of electron correlations on transport properties of iron at Earth's core conditions. *Nature* **517**, 605-U376, doi:10.1038/Nature14090 (2015).
6 Aubert, J., Tarduno, J. A. & Johnson, C. L. Observations and Models of the Long-Term Evolution of Earth's Magnetic Field. *Space Sci Rev* **155**, 337-370, doi:10.1007/s11214-010-9684-5 (2010).
7 Biggin, A. J., Strik, G. & Langereis, C. G. The intensity of the geomagnetic field in the late-Archaean: new measurements and an analysis of the updated IAGA palaeointensity database. *Earth Planets and Space* **61**, 9-22 (2009).
8 Biggin, A. J. & Paterson, G. A. A new set of qualitative reliability criteria to aid inferences on palaeomagnetic dipole moment variations through geological time. *Frontiers in Earth Science* **2**, 24, 21-29, doi:10.3389/feart.2014.00024 (2014).
9 Aubert, J., Labrosse, S. & Poitou, C. Modelling the palaeo-evolution of the geodynamo. *Geophys J Int* **179**, 1414-1428, doi:10.1111/j.1365-246X.2009.04361.x (2009).
10 Dunlop, D. J. & Yu, Y. in *Timescales of the internal geomagnetic field* Vol. 145 *Geophysical monograph series* (ed J. E. T. Channell) 85-100 (AGU, 2004).
11 Prévot, M. & Perrin, M. Intensity of the Earths Magnetic-Field since Precambrian from Thellier-Type Paleointensity Data and Inferences on the Thermal History of the Core. *Geophys J Int* **108**, 613-620 (1992).
12 Biggin, A. J. & Thomas, D. N. Analysis of long-term variations in the geomagnetic poloidal field intensity and evaluation of their relationship with global geodynamics. *Geophys J Int* **152**, 392-415 (2003).
13 Valet, J. P. Time variations in geomagnetic intensity. *Rev Geophys* **41**, 1004, doi:1010.1029/2001RG000104, doi:10.1029/2001RG000104 (2003).
14 Biggin, A. J., Strik, G. H. M. A. & Langereis, C. G. Evidence for a very-long-term trend in geomagnetic secular variation. *Nat Geosci* **1**, 395-398, doi:10.1038/Ngeo181 (2008).
15 Macouin, M., Valet, J. P. & Besse, J. Long-term evolution of the geomagnetic dipole moment. *Phys Earth Planet In* **147**, 239-246 (2004).
16 Tauxe, L. & Yamazaki, T. in *Geomagnetism* Vol. 5 *Treatise on Geophysics* (ed M Kono) Ch. 13, 510-563 (Elsevier, 2007).
17 Valet, J. P., Besse, J., Kumar, A., Vadakke-Chanat, S. & Philippe, E. The intensity of the geomagnetic field from 2.4 Ga old Indian dykes. *Geochem Geophy Geosy* **15**, 2426-2437, doi:Doi 10.1002/2014gc005296 (2014).
18 Evans, D. A. D. Proterozoic low orbital obliquity and axial-dipolar geomagnetic field from evaporite palaeolatitudes. *Nature* **444**, doi:10.1038/nature05203 (2006).
19 Veikkolainen, T., Evans, D. A. D., Korhonen, K. & Pesonen, L. J. On the low-inclination bias of the Precambrian geomagnetic field. *Precambrian Res* **244**, 23-32, doi:10.1016/j.precamres.2013.09.004 (2014).
20 Ziegler, L. B., Constable, C. G., Johnson, C. L. & Tauxe, L. PADM2M: a penalized maximum likelihood model of the 0-2 Ma palaeomagnetic axial dipole moment. *Geophys J Int* **184**, 1069-1089, doi:10.1111/j.1365-246X.2010.04905.x (2011).
21 Valet, J. P., Meynadier, L. & Guyodo, Y. Geomagnetic dipole strength and reversal rate over the past two million years. *Nature* **435**, 802-805 (2005).
22 Tauxe, L., Gee, J. S., Steiner, M. B. & Staudigel, H. Paleointensity results from the Jurassic : New constraints from submarine basaltic glasses of ODP Site 801C. *Geochem Geophy Geosy* **14**, 4718–4733, doi:10.1002/ggge.20282 (2013).

23 de Groot, L. V., Fabian, K., Bakelaar, I. A. & Dekkers, M. J. Magnetic force microscopy reveals meta-stable magnetic domain states that prevent reliable absolute palaeointensity experiments. *Nat Commun* **5**, Artn 4548, doi:10.1038/Ncomms5548 (2014).
24 Smirnov, A. V. & Tarduno, J. A. Thermochemical remanent magnetization in Precambrian rocks: Are we sure the geomagnetic field was weak? *J Geophys Res-Sol Ea* **110**, B06103 (2005).
25 Tarduno, J. A. & Smirnov, A. V. in *Timescales of the Paleomagnetic Field* Vol. 145 *Geophysical Monograph Series* (eds J. E. T. Channell, D.V. Kent, W. Lowrie, & J.G. Meert) 328 (AGU, 2004).
26 Biggin, A. J. *et al.* Possible links between long-term geomagnetic variations and whole-mantle convection processes. *Nat Geosci* **5**, 526-533, doi:10.1038/Ngeo1521 (2012).
27 Kulakov, E. V., Smirnov, A. V. & Diehl, J. F. Absolute geomagnetic paleointensity as recorded by similar to 1.09 Ga Lake Shore Traps (Keweenaw Peninsula, Michigan). *Stud Geophys Geod* **57**, 565-584, doi:10.1007/s11200-013-0606-3 (2013).
28 Thomas, N. An Integrated Rock Magnetic Approach to the Selection or Rejection of Ancient Basalt Samples for Paleointensity Experiments. *Phys Earth Planet In* **75**, 329-342, doi:10.1016/0031-9201(93)90008-W (1993).
29 Veikkolainen, T. & Pesonen, L. J. Palaeosecular variation, field reversals and the stability of the geodynamo in the Precambrian. *Geophys J Int* **199**, 1515-1526, doi:10.1093/Gji/Ggu348 (2014).
30 Hunt, S. A. *et al.* On the increase in thermal diffusivity caused by the perovskite to post-perovskite phase transition and its implications for mantle dynamics. *Earth Planet Sc Lett* **319**, 96-103, doi:DOI 10.1016/j.epsl.2011.12.009 (2012).

Acknowledgements: The authors thank Prof Trond Torsvik for organising the 7th Nordic Supercontinents Meeting and acknowledge financial support for this from the European Research Council (ERC Advanced Grant, 267631) and the Research Council of Norway through its Centres of Excellence funding scheme (CEED, 223272). Dr Jane Rees and Dr Lauren Waszek are thanked for relevant discussions. AB acknowledges funding from a NERC standard grant (NE/H021043/1). GAP acknowledges funding form an NSFC grant (41374072). LT acknowledges funding from an NSF grant (EAR 1345003).

Author Contributions: AB designed the study. AB, EP, LP, and TV assigned the Q_{PI} values. AB, RH, GP, LP, TV and LT wrote the paper. AB, GP, and TV analysed the data.

Author Information: Reprints and permissions information is available at www.nature.com/reprints. The authors declare no competing financial interests. Correspondence and requests for materials should be addressed to A. Biggin (biggin@liv.ac.uk).

Main figure legends

Figure 1: Fits of palaeointensity data by minimum Q_{PI} value to palaeomagnetic inclination patterns predicted by a dipole field. (a,b) Box-plots for all data in 30° inclination bins with minimum Q_{PI} values as shown. Horizontal lines are medians, boxes show the interquartile range (IQR), error bars show the full range excluding outliers (crosses) defined as being more than ±1.5 IQR outside of the

box. (c) Number of data (N), number of references N_{ref}, and model misfit (shading shows bootstrapped 95% uncertainties) versus minimum Q_{PI} value. Raw data is plotted in Extended Data Figure 6a.

Figure 2: Four different representations of V(A)DM versus age for all data with $Q_{PI} \geq 3$. (a): Bubble plot where size indicates Q_{PI} value. (b) Density plot of number of measurements. (c) Density plot of sum of Q_{PI} values. (d) Box plot after binning with an interval length of 200 Myr (number of data in each are given with the number of published studies in parentheses). See Figure 1 caption for an explanation of the box plot.

Figure 3: Box-plot and summary statistics for different time intervals comprising V(A)DM estimates with $Q_{PI} \geq 3$. N_{Data} refers to the number of V(A)DM estimates in each interval and N_{Ref} refers to the number of published studies that these are drawn from. $V(A)DM_{Med}$ and $V(A)DM_{IQR}$ refer, respectively, to the median and interquartile range of the V(A)DM estimates within each interval. See Extended Data Table 1 for further information including the effect of varying the minimum Q_{PI} value. See Figure 1 caption for an explanation of the box plot. Thick error bars indicate 95% confidence limits (from 10,000 bootstraps) on the median values.

METHODS

Data Selection

During the Nordic Supercontinents Workshop in Haraldvangen, Norway in October 2014, we updated the PINT database[7] to contain all published palaeointensity measurements from rocks older than 500 Myr at the site mean level and applied Q_{PI} criteria as set out in ref. 8 (see also http://qpi.wikispaces.com/). These are a set of 8 criteria based on same model of Q criteria[31] as widely used for palaeomagnetic poles but reformulated for palaeointensity measurements and applied at the site-mean level. The Q_{PI} value is the sum of the criteria met and is intended to comprehensively reflect the extent to which numerous known sources of bias to palaeointensity estimates have been reasonably guarded against.

An additional criterion "MAG" was added to the original 8 which stipulates that the associated raw measurement data must be publically available for scrutiny (the MagIC database - http://earthref.org/MAGIC/ provides the ideal venue for these). It was recently observed that TRM preserved in non-single domain grains can be meta-stable producing an additional potential source of bias to palaeointensity estimates[23]. A very recent study[32] has suggested that this bias could be towards either over- or under-estimation of the palaeointensity (depending on the magnetic history of the samples) but could be guarded against by applying sufficiently strict reliability criteria. Importation of the raw data into the MagIC database would allow this to be done at a future date.

A further change to the criteria outlined in ref. 8 is that, in order to meet the AGE criterion in this study, we required the maximum nominal uncertainty in the age estimate of the result to be less than or equal to 50 Myr.

For the purpose of testing the dipole relationship (Figure 1 and Extended Data Figure 6), we only accepted measurements of the palaeointensity which had associated directional data (also at the site mean level) derived from a minimum of 3 specimens with an associated Fisher precision parameter (k) > 10 and/or 95% cone of confidence (α_{95}) < 30°.

Significant correlations between palaeointensity and inclination were tested for using the Kendall tau rank correlation coefficient assessed at the 5% significance level. The one-tailed correlation was used to specifically test for a positive rank correlation, which would be expected for a dominantly dipolar field.

Virtual dipole moments (VDMs) Virtual axial dipole moments (VADMs) are calculated (in Am^2 expressed as ZAm^2 where the Zeta prefix is 10^{21}) using equation (1)

$$V(A)DM = \frac{4\pi r^3}{\mu_0} F(1 + 3cos^2\theta)^{-\frac{1}{2}} \qquad (1)$$

Where r is the radius of the Earth (6.371×10^6m), μ_0 is the permeability of free space (1.257×10^{-6} m kg s^{-2} A^{-2}) , F is the palaeointensity (in Tesla) and θ is the magnetic colatitude calculated using equation (2):

$$\theta = 90 - tan^{-1}(1/2 \ tan\ I) \qquad (2)$$

Where I is the site mean inclination for a VDM (i.e. assuming a dipole field) and I is the study mean inclination for a VADM (i.e. assuming an axial dipole field and a sufficient averaging of directional secular variation)

Monte Carlo Resampling Test

To further test the hypothesis that the MID period (~1300 – 2400 Ma) has V(A)DMs that are significantly lower than those of the EARLY (> 2400 Ma) and LATE (< 1300 Ma) periods we adopt a Monte Carlo (MC) resampling approach with 10,000 repetitions. For this, we consider the uncertainties in both the ages and V(A)DMs and therefore exclude data where no uncertainties are reported, which leaves a total of 183 results with $Q_{PI} \geq 1$. For each repetition, the age and V(A)DM of each result are resampled from normal distributions where the means are the reported mean values. The reported age uncertainties are taken to represent $2\sigma_{Age}$ errors where σ_{Age} is the standard deviation. For the V(A)DM standard deviations we use the unbiased estimate of the standard deviation of the distribution of V(A)DM means:

$$\sigma_{VADM} = t_{\left(1-\frac{0.32}{2};N-1\right)} \frac{VADM_{Err}}{\sqrt{N}} \qquad (3)$$

where t is the t-critical value for the 68th percentile (i.e., the standard deviation coverage interval for a normal distribution), $VADM_{Err}$ is the reported uncertainty, and N is the number of specimens used to estimate the mean. σ_{VADM} represents the V(A)DM distribution that would be obtained if were able to repeat the experiments multiple times. After all data have been resampled for a given repetition, the resampled data are split into the EARLY, MID and LATE periods and a one-tailed Kolmogorov-Smirnov (K-S) test for equality of distributions is performed.

We count the proportion of repetitions where we cannot reject the null hypothesis of the K-S test. This represents the proportion of repetitions where it is unlikely that the MID period V(A)DMs are lower than the other periods at the 5% significance level. The results for the test with various Q_{PI} thresholds are given in Extended Data Table 1.

Despite the reduced number of data, the resampling test, which accounts for data uncertainties, confirms a reduction in the average dipole moment up to $Q_{PI} \geq 3$. However, too few data, particularly for the MID period, are available to confirm this for $Q_{PI} \geq 4$-5.

New Likelihood Test

A potential problem with using general statistical tests to determine significance for palaeomagnetic data sets is that they do not account for potentially strong correlations that may occur between data that are typically sampled highly non-uniformly though time. Here we are attempting to isolate variations on the billion year timescale but need to consider the risk that observed differences in fact arise from over-sampling of periods of unusually high or low field geomagnetic intensity produced by shorter timescale variations. Specifically:

1. Mantle convection may change the heat flowing across the core-mantle boundary causing shifts in the dipole moment lasting tens of millions of years[26]
2. Secular variation, reflecting the intrinsic operation of the geodynamo may produce similar shifts lasting up to a few hundred kyr [21]

Our understanding of the above processes is incomplete even for recent times and is very poor for the Precambrian period with which we are concerned with in this study. Nevertheless, we designed a test which attempted to incorporate Process 2 by using a record of dipole moment variations for the last 2 million years[20] and, further, allowed this to be rescaled (producing variations in the long term average of up to a factor of 3) to account for Process 1. The test was later repeated allowing for variations of up to a factor of 6 and 12 from Process 1.

It is impossible to be certain whether our rescaled models are representative for the time periods being tested. Nevertheless, we point out that the minimum (5 ZAm^2), maximum (143 ZAm^2) and median (54 ZAm^2) values generated by them (utilising a factor of 3 variation for Process 1) do at least appear to be similar to those observed in the measured values that we are testing (figure 2). Also, the test outlined below compares relative rather than absolute differences; therefore a very good fit is not required.

For the purpose of the tailored likelihood test, we first assigned every measurement in our $Q_{PI} \geq 3$ subset to a “Mantle Group” and a “Secular Variation (SV) Group” (Supplementary Table 2).

- Each Mantle Group comprised results whose stated age was within 50 Myr of one another. Where estimates could be non-uniquely assigned to Mantle Groups, they were placed in with the estimates whose age was closest to their own.
- Each SV Group comprised results which had the same stated age. If results had the same age but were assigned different polarities, they were placed in separate SV groups.

The likelihood test estimated the probability of differences of the relative magnitude observed between the dipole moment distributions from two intervals (EARLY, MID and/or LATE) being arrived at by chance alone subject to simulated effects of processes 1 and 2 above. Firstly, for each real pair of datasets, the following were calculated:

a. The relative difference in the medians (expressed as a percentage of the smaller value)
b. The relative difference in the interquartile ranges (IQRs; expressed as a percentage of the smaller value)
c. The P-value associated with a Kolmogorov-Smirnov test for equality of distribution

Subsequently, these were compared to similar values produced by 2 pseudo-datasets which were of equal size to the real datasets and which contained identically sized and configured Mantle Groups and Secular Variation Groups. These pairs of pseudo-datasets were derived by 10,000 iterations of the following procedure (see example in Extended Data Figure 7):

1. For each Mantle Group, the PADM2M model[20] of dipole moment variations for the last 2 Myr was rescaled using a factor drawn at random from a uniform distribution with a range of 0.5 to 1.5 (or 0.375 to 2.25 for rescaling factor 6 and 0.25 to 3.00 for rescaling factor 12). This was done to incorporate variations that might plausibly arise from mantle forcing of the geodynamo into the test.
2. For each Secular Variation Group within the Mantle Group, a 200 kyr continuous sub-interval within the rescaled model was selected at random. This was done to allow for data from the same Secular Variation Group to be plausibly clustered in time.
3. For each measurement within the Secular Variation Group, a dipole moment estimate was randomly selected from within the sub-interval.

The likelihood of obtaining each of the values in a-c above by chance alone (P(Med), P(IQR) and P(KS) in Extended Data Table 1) was estimated by the fraction of the 10,000 randomly generated pseudo-datasets that produced differences of the same or larger magnitude in these values.

The likelihood of simultaneously obtaining such differences (P(all) in Extended Data Table 1) was estimated by the fraction of the 10,000 randomly generated pseudo-datasets which produced differences of the same or larger magnitude in all three of the values simultaneously.

RECENT Dataset

Our RECENT data-set consists of all measurements of V(A)DM in the PINT database at the site-mean level that are derived from rocks with a stated age between 1 and 500 Myr. The interval 0-1 Myr was excluded to minimise skewing of the dataset and estimates were further required to meet the following criteria:

(i) The Q_{PI} criterion STAT which stipulates that the number of sample palaeointensity measurements comprising the mean is ≥ 5 and that the associated standard deviation is ≤ 25% of the mean value.

(ii) The use of one of the following palaeointensity techniques: T+ (Thellier with pTRM checks), M+ (Microwave with pTRM checks), LTD-DHT Shaw or some combination of techniques including at least one of the above. This should ensure that all results meet the ALT criterion of the Q_{PI} set.

These criteria were chosen as they are two of the most important indications of reliability and can be easily applied to measurements in the PINT database without requiring that the original manuscript is rechecked. They should ensure that the RECENT dataset comprises measurements with associated Q_{PI} values of at least 2. Previous experience suggests that the vast majority of this dataset will also satisfy the AGE criterion and many will also satisfy others too. We therefore expect that the median Q_{PI} for the 218 estimates comprising the RECENT dataset to be either 3 or 4. Some 139 estimates had directional information meeting the requirements defined above and the palaeointensity – inclination relationship is plotted in Extended Data Figure 6b.

References from Methods

31 Van der Voo, R. The Reliability of Paleomagnetic Data. *Tectonophysics* **184**, 1-9 (1990).

32 Shaar, R. & Tauxe, L. Instability of thermoremanence and the problem of estimating the ancient geomagnetic field strength from non-single-domain recorders. *P Natl Acad Sci USA* (Submitted).

Extended Data Figure and Table Captions

Extended Data Figure 1: Four different representations of V(A)DM versus time for all data with $Q_{PI} \geq 1$. (a): Bubble plot where size indicates Q_{PI} value (b) Density plot of number of measurements. (c) Density plot of sum of Q_{PI} values. (d) Box plot after binning with an interval length of 200 Myr (number of data in each are given with the number of published studies in parentheses). See Figure 1 caption for an explanation of the box plot.

Extended Data Figure 2: Four different representations of V(A)DM versus time for all data with $Q_{PI} \geq 2$. (a): Bubble plot where size indicates Q_{PI} value (b) Density plot of number of measurements. (c) Density plot of sum of Q_{PI} values. (d) Box plot after binning with an interval length of 200 Myr (number of data in each are given with the number of published studies in parentheses). See Figure 1 caption for an explanation of the box plot.

Extended Data Figure 3: Four different representations of V(A)DM versus time for all data with $Q_{PI} \geq 4$. (a): Bubble plot where size indicates Q_{PI} value (b) Density plot of number of measurements. (c) Density plot of sum of Q_{PI} values. (d) Box plot after binning with an interval length of 200 Myr (number of data in each are given with the number of published studies in parentheses). See Figure 1 caption for an explanation of the box plot.

Extended Data Figure 4: Four different representations of V(A)DM versus time for all data with $Q_{PI} \geq 5$. (a): Bubble plot where size indicates Q_{PI} value (b) Density plot of number of measurements. (c) Density plot of sum of Q_{PI} values. (d) Box plot after binning with an interval length of 200 Myr (number of data in each are given with the number of published studies in parentheses). See Figure 1 caption for an explanation of the box plot.

Extended Data Figure 5: Box-plots for time intervals defined in main text and summarised in Supp. Table 3 comprising measurements with different minimum Q_{PI} values. See Figure 3 for $Q_{PI} \geq 3$ data and Figure 1 caption for an explanation of the box plot. Thick error bars indicate 95% confidence limits (from 10,000 bootstraps) on the medians.

Extended Data Figure 6: Raw Palaeointensity vs Inclination data shown with a best-fitting dipole for the four studied time intervals. Circle size indicates Q_{PI} value in (a).

Extended Data Figure 7: Examples of two pseudo-datasets produced by one iteration of the new likelihood test (see *Methods* section for details). Each of the V(A)DM estimates (red asterisks) are drawn from one of multiple 200 kyr long sub-intervals (blue lines) of Padm2m[21] (black line) which is rescaled by a random factor between 0.5 and 1.5. Data from the same Mantle Group are drawn from sub-intervals with the same rescaling to simulate the possible effects of mantle-forced variations. Data from the same Secular Variation Groups are drawn from the same 200 kyr sub-interval to simulate the possible effects of further temporal clustering. Panel (a) shows an example using the Mantle Groups and SV Groups of interval LATE and (b) shows the same for interval MID.

Extended Data Table 1: Summary results from the Monte Carlo resampling test (see *Methods* for details). N refers to the number of data (required to have quoted uncertainty values) used in each test.

Extended Data Table 2: Results of the tailored likelihood test applied to datasets in Supplementary Table 2 (see *Methods* section for details). P(Med) and P(IQR) refer to the estimated likelihoods of the observed differences in the medians and interquartile ranges arising by chance alone. P(K-S) is the same but refers to the given level of significance observed in the Kolmogorv-Smirnov test of equality for probability distributions. P(ALL) refers to likelihood of all three above likelihoods being met simultaneously by chance alone. Note that the LATE vs MID tests were repeated after excluding data from studies referred to in the main text in order the test the robustness of the observed differences. Note that the P(ALL) value actually increases as a result of excluding Ref. 28.

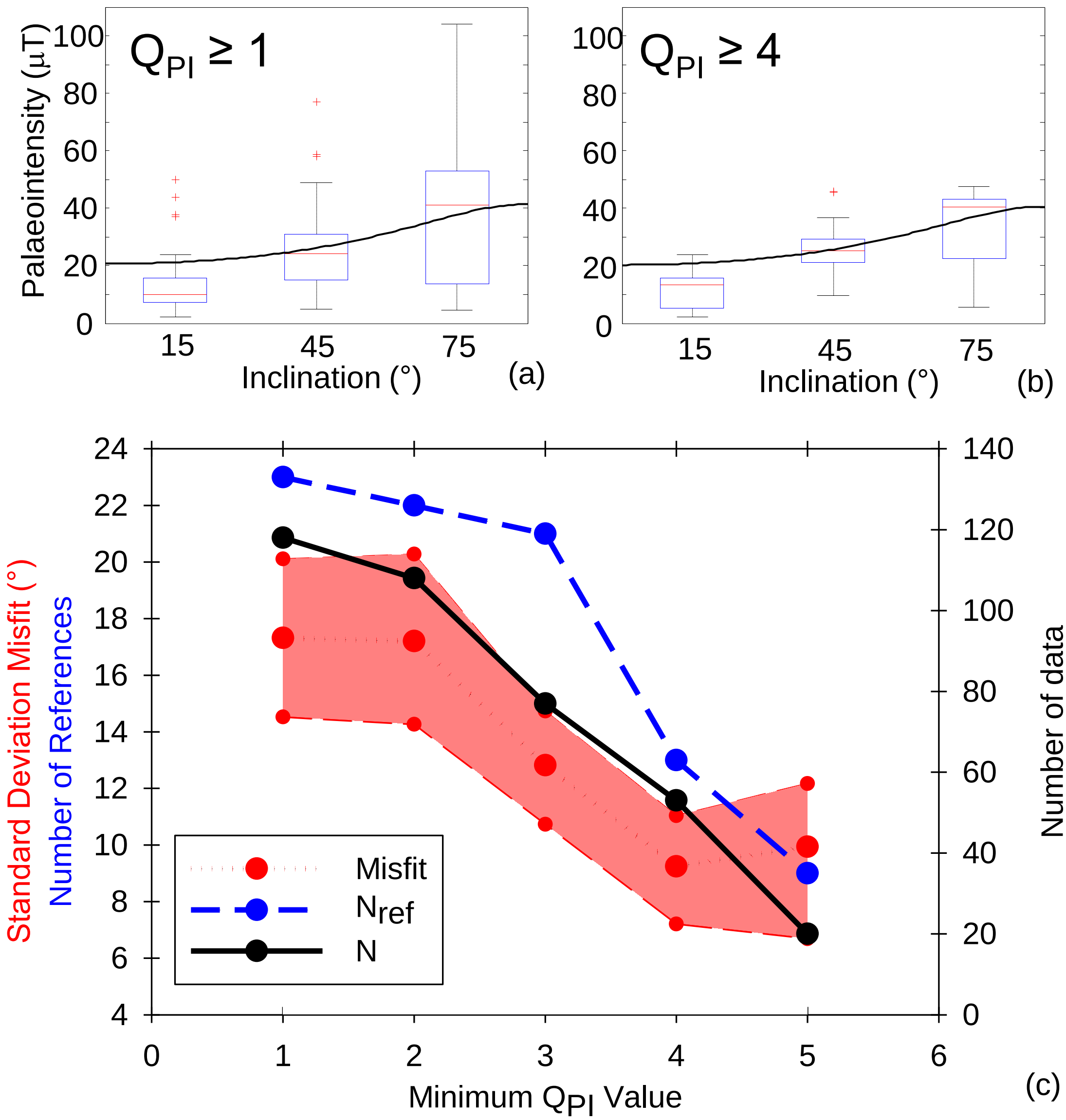

$Q_{PI} \geq 1$
Palaeointensity (μT)
Inclination (°)
(a)
$Q_{PI} \geq 4$
Inclination (°)
(b)
Standard Deviation Misfit (°)
Number of References
Number of data
Misfit
N_{ref}
N
Minimum Q_{PI} Value
(c)

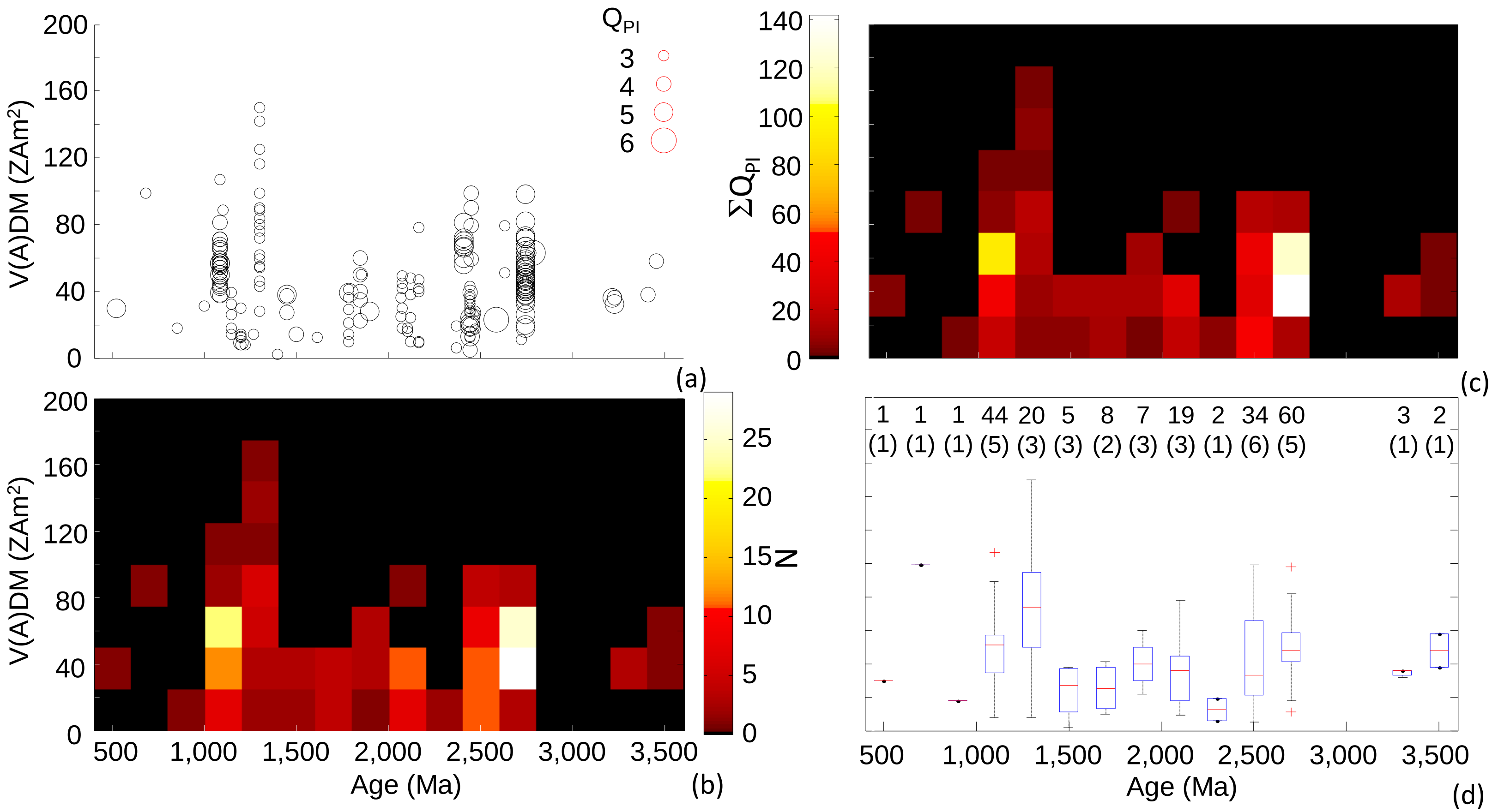

Q_{PI}
3
4
5
6
V(A)DM (ZAm²)
(a)
ΣQ_{PI}
(c)
V(A)DM (ZAm²)
N
Age (Ma)
(b)
1 1 1 44 20 5 8 7 19 2 34 60 3 2
(1) (1) (1) (5) (3) (3) (2) (3) (3) (1) (6) (5) (1) (1)
Age (Ma)
(d)

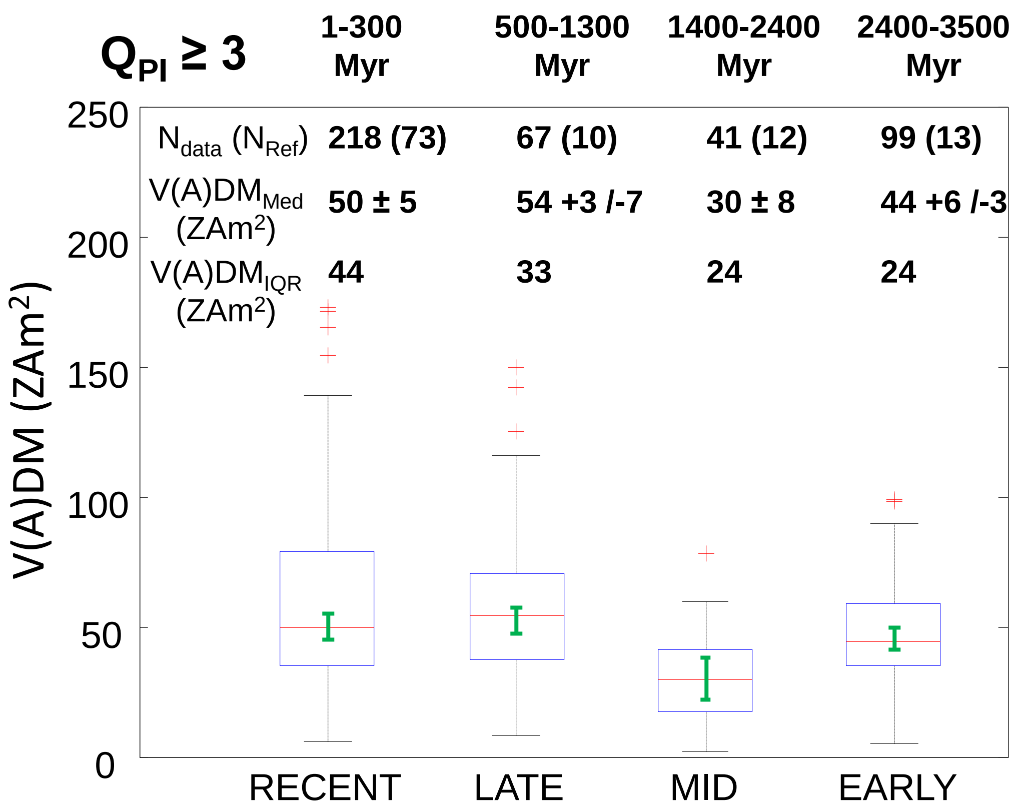

$Q_{PI} \geq 3$
1-300 Myr
500-1300 Myr
1400-2400 Myr
2400-3500 Myr
N_{data} (N_{Ref})
218 (73)
67 (10)
41 (12)
99 (13)
$V(A)DM_{Med}$ (ZAm^2)
50 ± 5
54 +3 /-7
30 ± 8
44 +6 /-3
$V(A)DM_{IQR}$ (ZAm^2)
44
33
24
24
V(A)DM (ZAm^2)
250
200
150
100
50
0
RECENT
LATE
MID
EARLY